



Original Article

Evaluation of hardening soil model on numerical simulation of behaviors of high rockfill dams

Pornthap Pramthawee, Pornkasem Jongpradist* and Warat Kongkitkul

*Department of Civil Engineering, Faculty of Engineering,
King Mongkut's University of Technology Thonburi, Thung Khru, Bangkok, 10140 Thailand.*

Received 20 August 2010; Accepted 24 June 2011

Abstract

With the continual increase in the height of concrete face rockfill dams constructed during this decade, the hyperbolic elastic model conventionally used in the numerical analyses of lower-height rockfill dams in the past practice becomes insufficient to reproduce the key responses of rockfills of high dam constructions and impoundments. This research aims at evaluating the ability of the elasto-plastic with isotropic hardening (HS) model for simulating more realistic responses in the analysis of high concrete face rockfill dams. The HS model and, for comparison, the hyperbolic elastic model are numerically implemented into a finite element program ABAQUS through the user subroutine to analyze the behaviors of rockfills under construction of a 182 m high dam. To obtain the reliable parameters in the analyses, the laboratory triaxial testing data of rockfills from actual construction are adopted and the calibration by model simulation is also conducted. The analysis results from both models are compared to the high-quality instrumented data of dam construction. It is proven that by using the HS constitutive model with the appropriately calibrated model parameters, the response of the rockfills under dam construction condition can be more accurately simulated.

Keywords: high rockfill dam, constitutive model, simulation, shear dilatancy, hardening soil model

1. Introduction

Compacted rockfill dams, which are embankment dam type structures, are gaining a worldwide recognition as the most economical and adaptive type of dams, particularly for regions with heavy rain where impervious soil reserves are insufficient. The concrete face rockfill dams (CFRDs) having upstream concrete slabs, which acts as a watertight element, are increasingly constructed in recent years as they are often the lowest-cost dam type. Understanding the behavior of rockfill dams is important for the design and safety evaluation. The main concern for the safety of CFRDs is the deformations of dam and the concrete face, which affect cracking

potential of concrete slab. Their behavior should be estimated realistically at both construction and reservoir filling stages. At present, the numerical approach by finite element method (FEM) or finite difference method (FDM) is mainly used to analyze the behavior of CFRDs. One of the key points in the analysis is selection of the constitutive model to reproduce the response of the rockfill materials under being loaded.

The heights of CFRDs which are under construction or have been recently completed are between 150 m and 300 m. With those heights, the rockfill materials in dams would be subjected by a broad stress range. The compaction of rockfills in thin layers during the construction results in density variation of rockfills. For such granular media, the stress and density dependent properties play an important role on its behaviors, particularly, the shear dilatancy behaviors of dense granular materials (Charles and Watts, 1980). The Hyperbolic Elastic model (HB) proposed by Duncan and

* Corresponding author.

Email address: pornkasem.jon@kmutt.ac.th

Chang (1970), which is commonly used in analysis of behavior of rockfill dams in past practice due to its convenience in implementation into finite element program and in obtaining the model parameters, seems to be no longer suitable for high CFRDs (Szostak-Chrzanowski *et al.*, 2008). In addition, due to the complicated construction procedures and the variation of storage water levels associated with high dams, the stress states of rockfill materials including loading, unloading, and reloading are more complex than those of rockfills in low-height dams. In this case, the elastic models are insufficient to describe the rockfill behaviors. These provoke the selection and development of more suitable models in deformation analysis of high CFRDs.

Recent studies related to the constitutive models for deformation analysis of CFRDs can be broadly classified into two main groups. The first one has paid an effort on getting better understanding of the behaviors of rockfills under high confining pressures and complex stress states by conducting laboratory tests (Huang *et al.*, 2007; Liu *et al.*, 2008) and has attempted to develop a more sophisticated model, mostly in the family of elasto-plastic model, such as disturbed state concept based model (Varadarajan *et al.*, 2003 and 2006) and strain hardening model (Xu and Song, 2009). The validation of the new proposed models is commonly done by comparisons between the model simulation and testing data from triaxial compression results. The other has paid the attention on evaluation of the available constitutive models on simulating the rockfill responses during construction and/or reservoir impounding of high CFRDs by comparing the simulation results with available measured data (Özkuzkiran *et al.*, 2006; Loupasakis *et al.*, 2009). The case studies were the completed dam constructions, where testing data of rockfill materials are either unavailable or incomplete. The parameters used in the analysis are then adapted from published information for similar materials and often only the rockfill modulus was used. Moreover, with the difficulties in numerical implementation, only less complicated models or models available in commercial programs were chosen. These issues indicate the gap between the model, the development of rockfills and model evaluation for analysis of high CFRDs.

The objective of the present work is to evaluate the efficiency of elasto-plastic model with strain hardening to simulate the high CFRD behaviors. The results are compared with the high quality testing data of rockfills from the actual dam construction site and quantitatively validated by the measured data at the dam site. The paper begins with considerations for the selection of the model, which include the sufficiency in reproducing the key behaviors and the ability to implement the model into a FEM program that is able to take the above-mentioned model into cooperation. However, for the sake of further possible analyses taking into consideration, for example, improvement of the constitutive model and extension of problem from 2D to 3D, a more general FEM program, which provides the user-defined features and flexibilities in modeling, should be selected. In this study, the FEM program ABAQUS (ABAQUS, 2008), which is widely

known for its flexibilities as mentioned above was used. The model is numerically implemented and then simulations are carried out to calibrate the model parameters with testing data. Then, the analysis of the construction of a high CFRD is performed and the analysis results are compared with the measured data. The comparisons with calibration and simulation results from HB model are also made to emphasize the necessity and highlight the impact of the selected model in analysis of high CFRDs.

2. Selection of Constitutive Models

As previously mentioned, the preferred model must be capable of reproducing the non-linear and inelastic stress-strain relationship, intense shear dilatancy behaviors of dense granular materials, and the stress-dependency of stiffness. Numerous models possessing a fair degree of these capabilities have been developed with various levels of complexity. Many of these models can only be employed by numerical experts and require special tests to obtain the model parameters. As a result, they are not widely adopted in engineering practice. From the mentioned concerns, the model based on the concept of isotropic strain hardening, which is proven to sufficiently predict the shearing characteristics of rockfills (Xu and Song, 2009) and can be easily implemented into FEM or FDM programs (Schanz *et al.*, 1999) is chosen. It is herein defined as Hardening Soil (HS) model. Brief explanation of the HS and HB model description are presented in the following sections. Both models are implemented by user-defined models within the subroutine UMAT in the ABAQUS program and then used to calibrate the model parameters with rockfill testing data and simulate the dam behaviors in the latter sections. The numerical formulation of model implementation is following the guidelines suggested by Schanz *et al.* (1999) and Dunne and Petrinic (2005).

2.1 Hyperbolic elastic model

The original model is proposed by Kondner (1963), developed and extended by Duncan and Chang (1970), which is commonly known as the "Duncan and Chang" Model. The hyperbolic stress-strain relationships were developed for use in nonlinear incremental analyses of soil deformation. The assumption is that a relationship between stress and strain is governed by the generalized Hooke's Law of elastic deformations. According to the suggestion of Kondner, the relationship between stress difference ($\sigma_1 - \sigma_3$) and axial strain (ε_a) can be described by a hyperbola. This hyperbola can be represented by an equation of the form:

$$\sigma_1 - \sigma_3 = \frac{\varepsilon_a}{\frac{1}{E_i} + \frac{\varepsilon_a}{(\sigma_1 - \sigma_3)_{ult}}} \quad (1)$$

where, σ_1 and σ_3 are the major and minor principal stresses; ε_a is the axial strain; E_i is the initial tangent modulus; $(\sigma_1 - \sigma_3)_{ult}$

is the asymptotic value of stresses difference. Duncan *et al.* (1980) described to outline the procedures, which used to determine hyperbolic relationships for finite element analyses of stresses and movements in soil masses. The main equations of HB model are:

Tangent modulus:

$$E_t = KP_a \left(\frac{\sigma_3}{P_a} \right)^n \left(1 - \frac{R_f (1 - \sin \varphi) (\sigma_1 - \sigma_3)}{2c \cos \varphi + 2\sigma_3 \sin \varphi} \right)^2 \quad (2)$$

Bulk modulus:

$$B = K_b P_a \left(\frac{\sigma_3}{P_a} \right)^m \quad (3)$$

Unloading modulus:

$$E_{ur} = K_{ur} P_a \left(\frac{\sigma_3}{P_a} \right)^n \quad (4)$$

Failure ratio:

$$R_f = \frac{(\sigma_1 - \sigma_3)_f}{(\sigma_1 - \sigma_3)_{ult}} \quad (5)$$

where P_a is the atmospheric pressure, c and φ are strength parameters, K is the modulus number, n is the modulus exponent, K_b is the bulk modulus number, m is the bulk modulus exponent, and K_{ur} is the unloading-reloading modulus number.

2.2 Hardening soil model

The hardening soil (HS) model is derived from the hyperbolic model of Duncan and Chang (1970), with some improvement on the hyperbolic formulations in an elastoplastic framework (Schanz *et al.*, 1999). This model is based on the Mohr-Coulomb failure criterion and contains two main types of hardening, namely shear hardening and volumetric hardening. According to this model, the hyperbolic relationships of standard drained triaxial tests tend to yield curves, which can be described by following:

$$-\varepsilon_1 = \frac{1}{2E_{50}} \frac{q}{1 - q/q_a} \quad \text{for: } q < q_f \quad (6)$$

where q_a is the asymptotic value of the shear strength, q is deviatoric stress, and ε_1 is vertical strain. The E_{50} represents for primary loading stiffness. The ultimate deviatoric stress, q_f derived from the Mohr-Coulomb failure criterion, and the quantity q_a in Equation 6 are defined as:

$$q_f = (c \cot \varphi - \sigma_3) \frac{2 \sin \varphi}{1 - \sin \varphi} \quad (7)$$

$$q_a = \frac{q_f}{R_f} \quad (8)$$

where R_f is the failure ratio.

2.2.1 Stiffness for primary loading

The parameter E_{50} is the confining stress dependent stiffness modulus for primary loading which can be described in Equation 9.

$$E_{50} = E_{50}^{ref} \left(\frac{c \cos \varphi - \sigma_3 \sin \varphi}{c \cos \varphi - p^{ref} \sin \varphi} \right)^m \quad (9)$$

For unloading and reloading, another stress dependent stiffness modulus is defined as:

$$E_{ur} = E_{ur}^{ref} \left(\frac{c \cos \varphi - \sigma_3 \sin \varphi}{c \cos \varphi - p^{ref} \sin \varphi} \right)^m \quad (10)$$

For oedometer conditions of stress and strain, the oedometer stiffness modulus E_{oed} for primary loading is:

$$E_{oed} = E_{oed}^{ref} \left(\frac{c \cos \varphi - \sigma_3 \sin \varphi}{c \cos \varphi - p^{ref} \sin \varphi} \right)^m \quad (11)$$

where p^{ref} is the reference pressure, E_{50}^{ref} is the secant stiffness modulus defined for a reference stress; m is the parameter that defines p^{ref} and minor principal stress, σ_3 , E_{50}^{ref} is the oedometer tangent stiffness modulus defined for a reference stress E_{ur}^{ref} . is the Young's modulus for unloading and reloading defined for a reference stress.

Both E_{50}^{ref} and E_{oed}^{ref} are necessary for the formulation of the hardening model. The E_{50}^{ref} controls the magnitude of the plastic strains associated with E_{50}^{ref} the shear yield surface. Similarly, E_{oed}^{ref} is used to control the magnitude of plastic strains originating from the yield cap.

2.2.2 Shear hardening

According to the proposal of Schanz *et al.* (1999), the shear yield function, f^s , can be defined as:

$$f^s = \frac{1}{E_{50}} \frac{q}{1 - q/q_a} - \frac{2q}{E_{ur}} - \gamma^p \quad (12)$$

$$\gamma^p = (2\varepsilon_1^p - \varepsilon_v^p) \approx -2\varepsilon_1^p \quad (13)$$

where ε_v is the plastic volumetric strain and γ^p is the hardening parameter. The HS model involves a relationship between $\dot{\varepsilon}_v^p$ and $\dot{\gamma}^p$. This flow rule has a linear form:

$$\dot{\varepsilon}_v^p = \sin \psi_m \dot{\gamma}^p \quad (14)$$

The mobilized dilatancy angle, ψ_m , and mobilized friction angle, φ_m , can be expressed by following equations (Schanz and Vermeer, 1996):

$$\sin \psi_m = \frac{\sin \varphi_m - \sin \varphi_{cv}}{1 - \sin \varphi_m \sin \varphi_{cv}} \quad (15)$$

$$\sin \varphi_m = \frac{\sigma_1 - \sigma_3}{\sigma_1 + \sigma_3 - 2c \cot \varphi} \quad (16)$$

At failure, the critical state friction angle, φ_{cv} , can be expressed as:

$$\sin \varphi_{cv} = \frac{\sin \varphi - \sin \psi}{1 - \sin \varphi \sin \psi} \quad (17)$$

where φ is the failure friction angle and ψ is the failure dilation angle. From definition of the flow rule, the plastic potential functions, g_s , can be expressed as:

$$g_s = q - M^*(p + c \cot \psi_m) \quad (18)$$

$$M^* = \frac{6 \sin \psi_m}{3 - \sin \psi_m} \quad (19)$$

and the shear yield locus can expand up to the ultimate Mohr-Coulomb failure surface.

2.2.3 Volumetric hardening

The second type of hardening model is cap-type yield surface, which accounts for volumetric hardening. This surface is introduced to close the elastic region in the direction of the p-axis. The cap yield function, f^c , and plastic potential function, g^c , are defined as:

$$f^c = g^c = \frac{q^2}{M^2} + (p + \cot \varphi)^2 - (p_p + c \cot \varphi)^2 \quad (20)$$

where

$$q = \sigma_1 + (\alpha - 1)\sigma_2 - \sigma_3 \quad (21)$$

$$p = \frac{\sigma_1 + \sigma_2 + \sigma_3}{3} \quad (22)$$

$$\alpha = \frac{3 + \sin \varphi}{3 - \sin \varphi} \quad (23)$$

The hardening law relating p_p to the volumetric cap strain ε_v^c is:

$$\varepsilon_v^c = \frac{H}{m+1} \left(\frac{p_p}{p^{ref}} \right)^{m+1} \quad (24)$$

The volumetric cap strain is the plastic volumetric strain in isotropic compression. Both H and M are cap parameter, which relate to E_{oed}^{ref} and K_0^{NC} , respectively. The shape of the cap yield is an ellipse in p - q plane which has length p_p on the p-axis and Mp_p on the q axis. The cap yield surface expands as a function of the pre-consolidation stress p_p .

3. Rockfill Materials and Model Calibration

3.1 Rockfill materials

The experimental data from the specialized tests of the rockfill materials from dam construction is adopted (IWHR, 2007). Two kinds of blended materials of sandstone and siltstone were used. Laboratory tests of rockfill materials include the triaxial tests and compression tests. The gradation curves of the original materials and test samples are shown in Figure 1. For triaxial testing, the scaling down of original materials by the combination of Equivalent Quantity Replacement and Similar Particle Distribution Methods (IWHR, 2007) is used to prepare the testing samples. A dry unit weight of 21.0-21.5 kN/m³ is adopted to control the compaction of samples. The confining pressure used in the test ranges from 0.5 to 2.0 MPa. Two examples of the triaxial compression test results of rockfills for four main zones (details on rockfill zones will be explained in section 4.1) shown as circular markers are illustrated in Figures 2 and 3. The nonlinear stress-strain relationships are obviously seen for all type of rockfills and the shear dilatancy at low confining pressures starts from low shear strain (3-7%) except that for zone 3C&3E.

3.2 Model calibration

The procedure for determination of the model parameters are referred to Duncan *et al.* (1980) for HB model and Schanz *et al.* (1999) for HS model. However, after using the obtained parameters to numerically predict the stress-strain behaviors of rockfills and compare with testing results, some discrepancy can be clearly noticed. The parameters are then adjusted to improve the prediction. Since the horizontal stresses computed from analysis of dam construction (next section) cover the range not over than 1.5 MPa, the calibra-

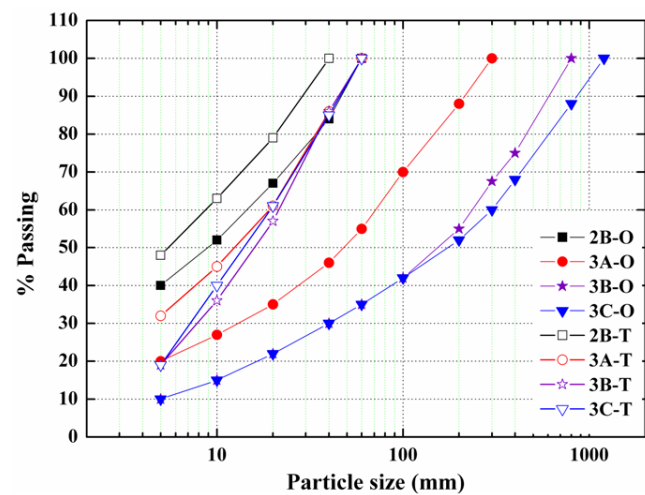


Figure 1. Gradation curves of the original materials and test samples.

tion is then paid attention to principally best fit the curves of confining pressures of 0.5, 1.0, and 1.5 MPa. The calibration is done in a way that the deviator stress-axial strain curves of those predicted by both models are as close as possible with testing data. The parameters from calibration which are used in simulation hereafter are listed in Tables 1 and 2 for HB and HS models, respectively. The predictions by the two models from calibrated parameters are shown by solid and dashed lines in Figures 2 and 3 together with testing results. From comparison between the predicted and actual testing results of four rockfill types, in general, the numerical simulations of both models predict the deviator stress-axial strain and volumetric strain-axial strain curves fairly well for each type of rockfill. However, there is more discrepancy between the simulated and testing results for volumetric strain-axial strain curves, particularly those of HB model. Moreover, as expected, the discrepancy of simulated volumetric strain from HB model at low confining pressure becomes more pronounced.

4. Dam Characteristics and Data for Analysis Case

4.1 Dam characteristics

The construction of the dam in this study was started in 2006 and has just finished in March 2010. The dam will be fully operated in 2013. The first impoundment is now being conducted. Therefore, this study covers only the analysis of dam construction. The gross storage volume of the reservoir is 2,440 million cubic meters. The dam is CFRD type with the height of 182.0 m. The lowest foundation level is at 199.0 m above sea level (asl), and the crest elevation is at 381.0 m asl. The maximum water level is 375.0 m asl. This dam is classified as very high dam in a narrow valley consisting of compacted rockfill found on a rock foundation, plinth, concrete face-slab and wave wall. The slopes of dam are 1.4 H:1.0 V on both upstream and downstream. The geological formation at the dam site generally consists of cliff-forming sandstone, interbedded clay-stone, siltstone, and conglomerate of Jurassic-

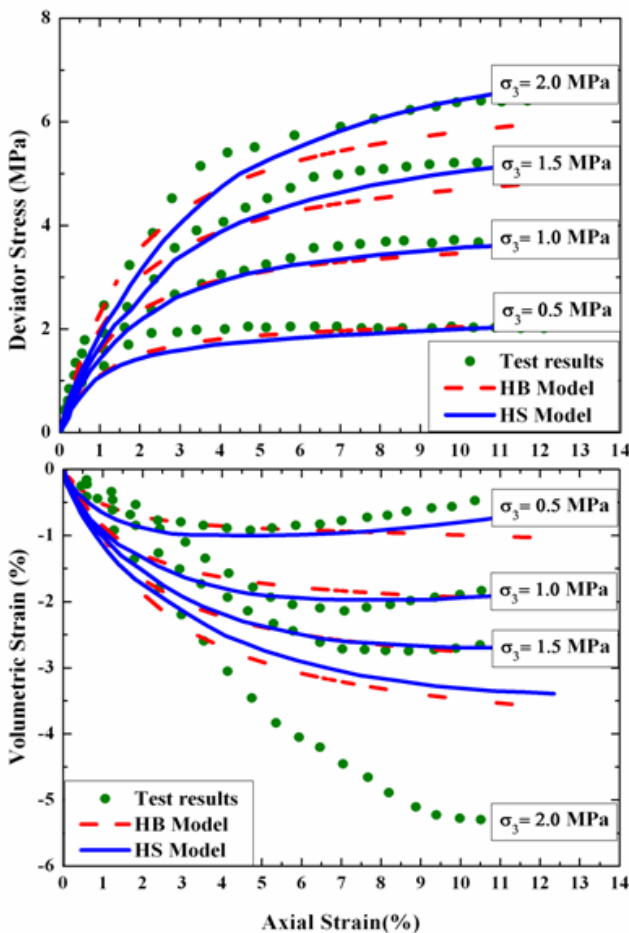


Figure 2. Calibrated results between simulation and CD-triaxial tests of zone 3B&3D (negative indicates compression).

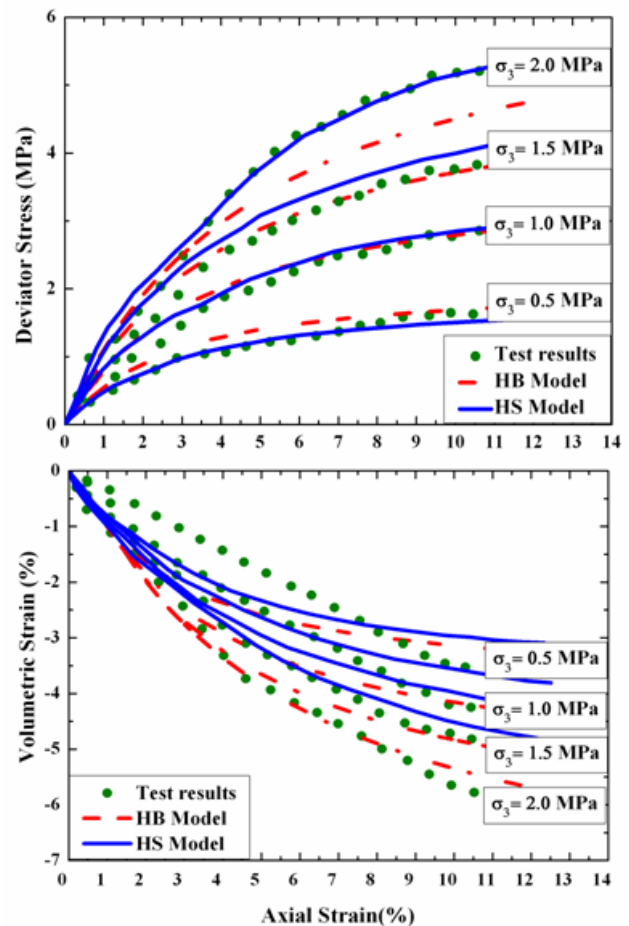


Figure 3. Calibrated results between simulation and CD-triaxial tests of zone 3C&3E (negative indicates compression).

Table 1. Material parameters for the hyperbolic elastic model.

Parameters	Dam Zoning			
	2B	3A	3B&3D	3C&3E
K	1600	1050	1000	330
K_{ur}	3200	2100	2000	660
K_b	2000	900	1100	110
n	0.38	0.32	0.38	0.45
m	-0.27	-0.05	-0.29	0.28
c	0	0	0	0
φ_0°	44.10	45.90	46.5	42.9
$\Delta\varphi^\circ$	1.50	3.00	3.2	3
R_f	0.98	0.82	0.864	0.751
P_a (kPa)	101.40	101.40	101.4	101.4

Table 2. Material parameters for the hardening soil model.

Parameters	Dam Zoning			
	2B	3A	3B&3D	3C&3E
c (kPa)	1	1	1	1
φ_0°	42	42	42	41
$\Delta\varphi^\circ$	2	2	2	1
E_{50}^{ref} (kPa)	90000	85000	100000	16000
E_{oed}^{ref} (kPa)	90000	85000	80000	14000
m	0.40	0.30	0.18	0.65
E_{ur}^{ref} (kPa)	270000	255000	300000	48000
n	0.20	0.20	0.20	0.2
p^{ref} (kPa)	100	100	100	100
K_0	0.33	0.33	0.33	0.34
R_f	0.90	0.90	0.90	0.90

Cretaceous age, and Quaternary deposits. Zoning of dam are classified into three designated zones. Zone 1 (1A and 1B) is concrete face slab protection zone in the upstream of face slab. Zone 2 (2A and 2B) is concrete face-slab supporting zone in the downstream of face slab. Zone 3 (3A, 3B, 3C, 3D and 3E) is the rockfill zone, which is the major part of the rockfill materials. The configuration of the dam and the construction sequences are shown in Figure 4.

4.2 Instrumentation

The instrumentation system for the dam was installed for monitoring the behavior of dam. The instrumentations include total pressure cells (TPC), fixed embankment extensometers (FEE), hydrostatic settlement cells (HSC), probe inclinometer (PI), settlement gauge (SG), and vibrating-wire piezometers (VWP). The monitoring results used in comparison with analyzed results in this study include settlements from HSC at elevations of 259.0 and 319.0 m asl and SG on downstream side and lateral movement from PI on down-

stream side. The locations of the installations are also illustrated in Figure 5.

5. Analysis and Evaluation

5.1 Limitations

The finite element program ABAQUS is employed throughout this analysis. The simulations have been carried out as 2-D plane strain of largest cross-section of the dam at which the instrumented data are available. Zones 1A, 1B, and 2A are not expected to have a significant effect on the whole dam behavior and have not been included in this analysis. The concrete membrane and a parapet wall are also not modeled. In this analysis, the rock foundation is assumed to be rigid. Therefore, at the foundation level, the stress-strain and the movements are not computed. In the analysis, the result of the simulation by both soil models will be compared and evaluated in terms of stresses and displacements in rockfill dam. For comparing with the instrumentation records during construction, the moment of completion of referred construction stage is considered. Since the chosen models do not take into account the time dependent behavior or creep of material, therefore, the settlement from creep is not taken into account.

5.2 Finite element models

The embankment is modeled by 3-node triangular and 4-node quadrilateral solid elements. The finite element mesh is shown in Figure 5. This mesh consists of 1,471 elements and 1,377 nodes. The material parameters used are those shown in Table 1 and 2. The unit weights of rockfills are 21 kN/m³ for Zone 3C&3E and 21.5 kN/m³ for other zones. The construction loading of embankment is simulated by 77 steps for end of construction (EOC) that have about 5-m thick layers.

5.3 Results of the computation at the end of construction

Examples of the contours of the computational results are shown in Figure 6 and 7, and a summary of the computational results for maximum value is shown in Table 3. The maximum vertical stress occurred at base of the dam, and the value from HB model is slightly larger than that from the HS model. In contrast, the maximum horizontal stress computed from HS model is larger than that of the HB model.

The maximum settlement of rockfill simulated from both models occurs in zone 3C at downstream side as shown in Figure 6 because the stiffness of rockfill in zone 3C is lower than those in zones 3B and 3D. The settlement distribution has a similar tendency but significantly different magnitude. From the figure, it is seen that the HB model gives much higher predicted values of maximum settlement compared to those from the HS model.

Distribution of horizontal displacement of the dam is

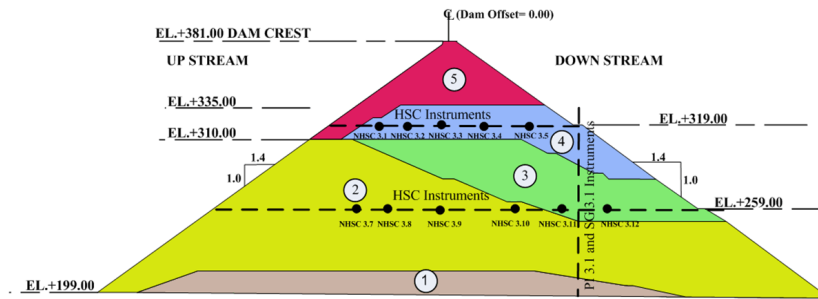


Figure 4. Configuration, construction sequences, and locations of instruments at the dam site.

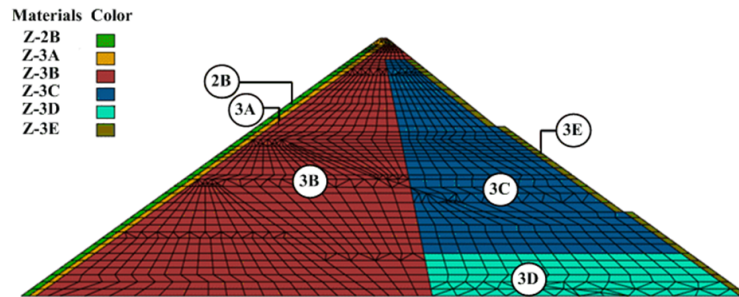


Figure 5. Zones of rockfill and finite element mesh used in the analyses.

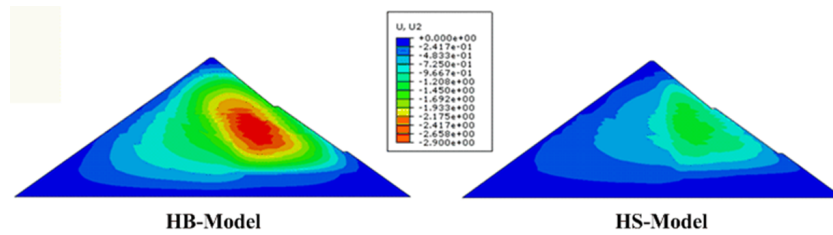


Figure 6. Vertical displacement in meter for EOC (negative indicates settlement).

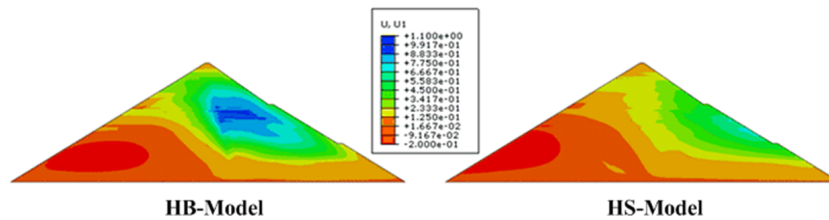


Figure 7. Horizontal displacement in meter for EOC (upstream is negative).

not symmetrical to the dam axis for both models as can be perceived in Figure 7. The maximum value at the downstream is larger than that at the upstream. At upstream, the computed maximum horizontal displacement from the HS model is larger than that from the HB model and towards upstream direction. On the other hand, the maximum horizontal displacement at the downstream side computed from the HB model is larger

than that from the HS model.

From the described comparisons, it is clear that the two models reproduce different behaviors in terms of magnitude of deformations although the parameter set used in the analyses could simulate similar deviatoric stress-axial strain curves. This indicates the significance of the volumetric term in material modeling for analysis of high CFRD.

Table 3. Comparison of the maximum value of the computational results of the end of construction stage (EOC).

Items	Computation	
	HB model	HS model
Settlement (mm)	2,861	1,444
Horizontal displacement towards upstream (mm)	147.3	184.1
Horizontal displacement towards downstream (mm)	1,066	693.2
Vertical stress (kPa)	3,380	3,157
Horizontal stress (kPa)	1,210	1,471

5.4 Comparisons with instrumented data

In order to ensure the ability of the model to quantitatively simulate the behavior of rockfill, the evaluations are performed by comparing the analysis results with the available monitoring recordings. The settlements of rockfills from HSC instruments set are shown in Figures 8(a) and (b) together with the predicted results from both models. From the comparisons, the predicted values from HS model are smaller than the monitoring results. In contrast, the HB model generally gives higher values. This may be attributed from foundation settlement of dam whereas the foundation is assumed to be rigid for simulation. Also, the breakage of the particles and time-dependent deformation and creep may occur in rockfills. It is noted that the dam construction is principally a 3D problem, in particular, when the dam width is not significantly larger than the dam height. Simplification of 3D to 2D might be a source of this discrepancy as well. The comparison of predicted values and measured settlements of rockfills from SG-3.1 instruments is shown in Figure 9. This also indicates that the predicted values from HB model from elevation +230.0 m asl to the dam crest are much larger than the measured ones. In particular, at the elevation +280.0 m asl, the predicted value is 2.5 times larger than the measured value. On the other hand, the predicted values from HS model are in good agreement with measured data for the entire recorded elevations.

The measured horizontal displacement distribution along the elevation from PI-3.1 in downstream side is also shown in Figure 9 together with the predicted values. It is reaffirmed that the predicted values from HS model, although larger, are in good agreement with measured data for the entire recorded elevations while the predicted values from the HB model are much larger.

From the comparisons with monitoring results of both instruments, the settlements and horizontal displacements predicted by the HS model are much close to the monitoring results than those by the HB model, in spite of using the model parameters which are adjusted to simulate similar deviator stress-strain curves. This indicates the necessity of considering the volumetric strain and shear dilatancy in

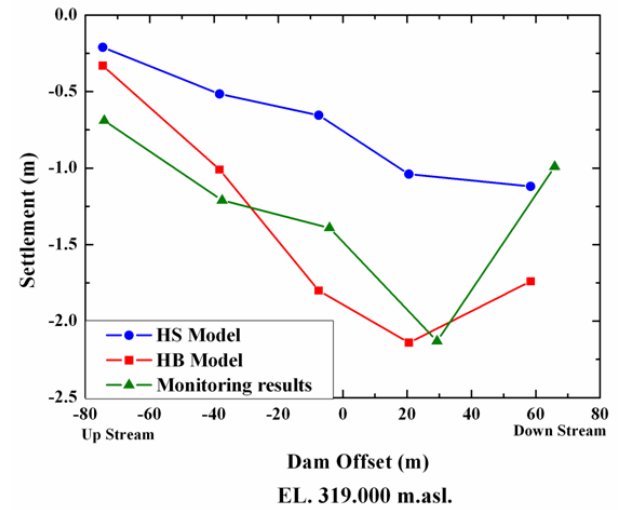
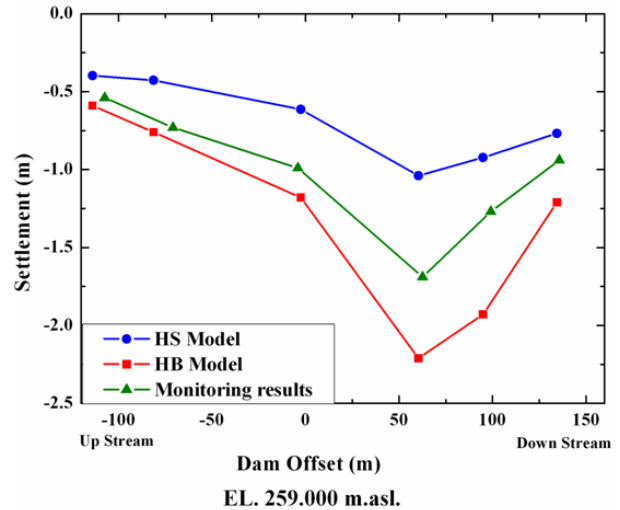


Figure 8. Settlements of rockfill by HSC instruments set.

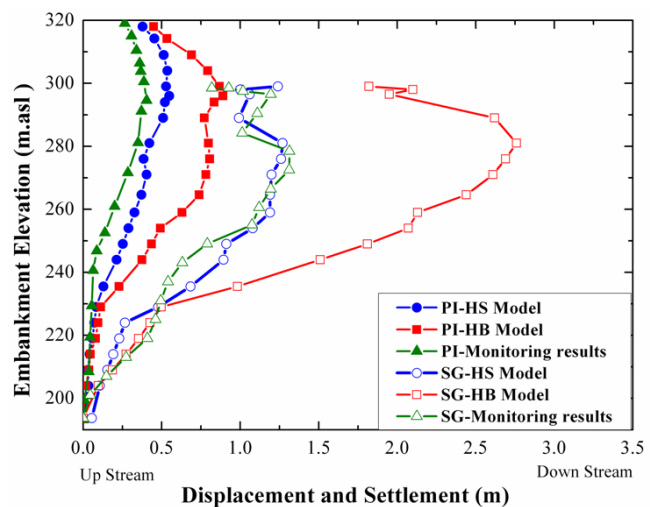


Figure 9. Settlements and horizontal displacement of rockfill varied level in embankment by SG 3.1 and PI-3.1 instruments sets, respectively.

modeling the rockfills in the analysis of high CFRDs. The elasto-plastic with isotropic hardening model evaluated in this study can highly improve the effectiveness of prediction of CFRD deformation at the end of construction. The model can also be used in the analysis of CFRD construction. To enhance the confidence of using the model, the validation of analysis results with the measured data for reservoir impounding condition should be performed.

5. Conclusions

The key behaviors of dense granular materials governing the deformation behaviors of high CFRDs are reviewed. The selected isotropic hardening model, so-called hardening soil model (HS), and the hyperbolic elastic model (HB) have been numerically implemented into the FEM program to simulate the deformation behaviors of a 182 m high CFRD using the calibrated model parameters from actual testing results of construction materials. The evaluation of the model ability in reproducing the rockfill behaviors is performed by comparing the simulated results with those from CD-triaxial tests and measured in-situ data. The comparisons emphasize the necessity and impact of the selection of the model for analysis of a high CFRD.

From the results of the study, it can be deduced that:

(1) The values of the required parameters for both soil models, which derived from experimental results, shall be calibrated by back analysis in FEM. The HS model can simulate the behaviors of rockfill and back analysis triaxial tests with better agreement than the HB model, particularly, in terms of volumetric strain and shear dilatancy.

(2) The computed results from 2-D plane strain condition analyzed by using the HS model are found to be in relatively better agreement with the in-situ reading than the HB model.

(3) At the end of construction stage, the displacement magnitude from the simulation by using the HS model is less than that from the HB model because the volumetric dilatancy behavior occurs in rockfill. In theory, the dilatancy behavior has an influence on the volumetric strain for real behavior of dense sand. Therefore, the HS model is more suitable in representing the rockfill behavior than the HB model, especially for the analysis of high rockfill dam.

The study indicates that the hardening soil model is more appropriate for analysis of the behavior of high rockfill dams than the hyperbolic elastic model commonly used for low-height rockfill dams. The analysis with HS model can be used to predict the performances of high CFRDs for end-of-construction condition with some confidence. However, the study is limited to only the construction stage. Future study for reservoir filling condition will enhance the confidence.

Acknowledgement

The authors gratefully acknowledge the Geotechnical and Foundation Engineering Company Limited (GFE) for

support on observed data. The authors are grateful for financial supports from the Thailand Research Fund (TRF) and GFE under TRF-master research grant (MAG Window I) MRG-WI525E084.

References

- ABAQUS, 2008. Version 6.7, Dassault Sytemes Simulia Corp.
- Charles, J.A. and Watts, K.S. 1980. The influence of confining pressure on the shear strength of compacted rockfill. *Geotechnique*. 30(4), 353-367.
- Duncan, J.M. and Chang, C.Y. 1970. Nonlinear Analysis of Stress and Strain in Soils. *Journal of Soil Mechanics and Foundation Division, American Society of Civil Engineers (ASCE)*. 96(5), 1629-1653.
- Duncan, J.M., Byrne, P., Wong, K.S. and Mabry, P. 1980. strength, Stress-Strain and Bulk Modulus Parameters for Finite Element Analyses of Stresses and Movements in Soil Masses, Report No. UCB/GT/80-01, Office of Research Services University of California, Berkeley California, pp. 20-49.
- Dunne, F. and Petrinic, N. 2005. Introduction to Computational Plasticity. Oxford series on materials modelling, Oxford University Press, pp 169-176.
- Huang, W., Ren, Q. and Sun, D. 2007. A Study of Mechanical Behavior of Rockfill Materials with Reference to Particle Crushing. *Science in China, Series E: Technological Sciences*. 50 (suppl. 1), 125-135.
- IWHR. 2007. Report on Laboratory Tests of the Rockfill Materials of Nam Ngum 2 CFRD in Laos. Department of Geotechnical Engineering, Institute of Water Resource and Hydropower Research (IWHR), China, May 2007, pp 1-36.
- Kondner, R. L. 1963. Hyperbolic Stress-Strain Response: Cohesive soils. *Journal of Soil Mechanics and Foundation Division, American Society of Civil Engineers (ASCE)*. 89(1), 115-143.
- Liu, H., Deng, A. and Shen, Y. 2008. Shear Behavior of Coarse Aggregates for Dam Construction under Varied Stress Paths. *Water Science and Engineering*. 1(1), 63-77.
- Loupasakis, C.J., Christaras, B.G. and Dimopoulos, G.C. 2009. Evaluation of Plasticity Models' Ability to Analyze Typical Earth Dams' Soil Materials. *Journal of Geotechnical and Geological Engineering*. 27, 71-80.
- Özkuzukiran, S., Özkan, M.Y., Özyaziciođlu, M., and Yildiz, G.S. 2006. Settlement behavior of a concrete faced rockfill dam. *Journal of Geotechnical and Geological Engineering*. 24, 1665-1678.
- Schanz, T. and Vermeer, P.A. 1996. Angles of Friction and Dilatancy of Sand. *Geotechnique*. 46(1), 145-151.
- Schanz, T., Vermeer, P.A. and Bonnier, P.G. 1999. The Hardening Soil Model: Formulation and Verification. *Beyond 2000 in Computational Geotechnics-10 years of Plaxis*, Balkema, Rotterdam, pp. 281-96.
- Szostak-Chrzanowski, A., Deng, N. and Massiera, M. 2008. Monitoring and Deformation Aspects of Large Con-

- crete Face Rockfill Dams. 13th International Federation of Surveyors (FIG) Symposium on Deformation Measurement and Analysis, Lisbon, Portugal, May 12-5, 1-10.
- Varadarajan, A., Sharma, K.G., Venkatachalam, K. and Gupta, A.K. 2003. Testing and Modeling Two Rockfill Materials. *Journal of Geotechnical and Geoenvironmental Engineering*. 129(3), 206-218.
- Varadarajan, A., Sharma, K.G., Abbas, S.M. and Dhawan, A.K. 2006. Constitutive Model for Rockfill Materials and Determination of Material Constants. *International Journal of Geomechanics*. 6(4), 226-237.
- Xu, M. and Song, E. 2009. Numerical Simulation of the Shear Behavior of Rockfills. *Computers and Geotechnics*. 36 (8), 1259-1264.